Article ID: 1000-324X(2021)02-0197-06 **DOI:** 10.15541/jim20200126

High Temperature Interfacial Stability of Fe/$Bi_{0.5}Sb_{1.5}Te_3$ Thermoelectric Elements

WANG Xu[1,2], GU Ming[1], LIAO Jincheng[1], SONG Qingfeng[1], SHI Xun[1], BAI Shengqiang[1], CHEN Lidong[1,2]

(1. State Key Laboratory of High Performance Ceramics and Superfine Microstructure, Shanghai Institute of Ceramics, Chinese Academy of Sciences, Shanghai 201899, China; 2. Center of Materials Science and Optoelectronics Engineering, University of Chinese Academy of Sciences, Beijing 100049, China)

Abstract: The high temperature interfacial stability of thermoelectric (TE) elements, which is mainly evaluated by the inter-diffusion and interfacial resistivity at the interface between the barrier layer and the TE material, is one of the key factors determining the service performance and application prospects of TE devices. In this study, a screening method based on high-throughput strategy was employed to further improve the interfacial stability of P-type bismuth telluride TE devices, and Fe was proved the preferred barrier layer material for P-type $Bi_{0.5}Sb_{1.5}Te_3$ (P-BT). Then Fe/P-BT TE elements were prepared by one-step sintering. Evolution of the Fe/P-BT interfacial microstructure during high temperature accelerated aging was systematically studied, and stability of the interfacial resistivity was explored. It is found that during aging, the Fe/P-BT interface is well bonded and the composition of the ternary Fe-Sb-Te diffusion layer remains basically unchanged. The diffusion layer thickness increases linearly with the square root of the aging time and the growth activation energy is 199.6 kJ/mol. The initially low interfacial resistivity of the Fe/P-BT interface increases slowly with the prolonged aging time but remains below 10 $\mu\Omega\cdot cm^2$ even after 16 d at 350 ℃. The life prediction based on the interfacial diffusion kinetics indicates that Fe is a suitable barrier layer material for $Bi_{0.5}Sb_{1.5}Te_3$ TE elements.

Key words: thermoelectric element; bismuth telluride; barrier layer; interfacial diffusion; interfacial resistivity

Energy shortage is becoming increasingly prominent. On the other hand, every year more than 60% of the global energy consumption eventually dissipates into the environment in the form of waste heat[1-2]. With the advantages of no moving parts and no emission, thermoelectric (TE) power generation can convert heat directly into electricity based on the Seebeck effect, which can be applied in the field of waste heat recovery[3-6]. The theoretical conversion efficiency limit of TE devices mainly depends on the performance of TE materials, which is usually presented by the dimensionless figure of merit zT ($zT=S^2\sigma T/\kappa$, where S, σ, T, and κ are the Seebeck coefficient, electrical conductivity, absolute temperature, and thermal conductivity, respectively). In the low and medium temperature range (room temperature to 300 ℃), the most commonly used TE materials are bismuth telluride (BT) based alloys with the zT of 1.0–1.5[7-10].

The TE device is usually composed of multiple TE couples connected electrically in series and thermally in parallel. Each TE couple owns one P-type and one N-type element, connected with the electrodes. The interface between the electrode and the TE material is usually the weakest part of the TE device[11-13]. With the working temperature increasing or the service time prolonging, the inter-diffusion at the interface causes changes of the microstructure and chemical composition on both sides, which affects the interfacial strength, the interfacial resistivity and the material's TE properties. Meanwhile, the continuously increasing interfacial resistivity between the electrode and the TE material causes additional energy loss, which deteriorates the service performance of the TE device[14-16]. To suppress the interfacial diffusion and improve the interfacial stability,

Received date: 2020-03-10; **Revised date:** 2020-04-10; **Published online:** 2020-05-10
Foundation item: National Key Research and Development Program of China (2018YFB0703604); National Natural Science Foundation of China (51632010, 51972324)
Biography: WANG Xu(1994–), male, Master candidate. E-mail: wangxu@student.mail.sic.ac.cn
王 旭(1994–), 男, 硕士研究生. E-mail: wangxu@student.mail.sic.ac.cn
Corresponding author: BAI Shengqiang, professor. E-mail: bsq@mail.sic.ac.cn
柏胜强, 正高级工程师. E-mail: bsq@mail.sic.ac.cn

a barrier layer is required between the electrode and TE material[17-18].

Various efforts have been made to study the barrier layer and improve the interfacial stability of bismuth telluride TE devices. Currently, Ni is the most widely used barrier layer material for BT devices[19]. Chen, *et al.*[20] found Ni barrier layer can significantly reduce 32% of the interfacial resistivity by effectively suppressing the diffusion of Te and Sb on the border of $Bi_2Te_{2.5}Se_{0.5}$ and solder. Chen, *et al.*[21] observed different $NiTe_x$ phases generated at P-type $Ni/(Bi_{0.25}Sb_{0.75})_2Te_3$ and N-type $Ni/Bi_2(Te_{0.9}Se_{0.1})_3$ interfaces. At the temperature lower than 200 ℃, Ni/BT elements usually present low interfacial resistivities (<10 $\mu\Omega\cdot cm^2$). However, Liu, *et al.*[22] observed accelerated inter-diffusion between Ni and BT materials at the temperature higher than 200 ℃, which caused abnormal increase of the interfacial resistivity. To suppress the high temperature inter-diffusion, great efforts have been carried out to search for an improved barrier layer, including Ni-based alloys[23-25] and other binary[26-29] or ternary alloys[30]. Even though some of these selected barrier layer materials show effective resistance on interfacial diffusion, unfortunately still no candidate can synchronously provide low interfacial resistivity and high stability.

The traditional way to develop barrier layer for TE device is essentially a serial try-and-error searching work with heavy workload and low efficiency. In this study, an efficient screening method based on high-throughput strategy[31] was employed, and Fe was swiftly selected as the preferred barrier layer material for P-type $Bi_{0.5}Sb_{1.5}Te_3$ (P-BT) from 6 candidates (Cr, Co, Ti, Fe, Zr, Al). Fe/P-BT TE elements were then prepared and aged. The evolution of the interfacial microstructure was analyzed, and the interfacial resistivity was investigated. Finally, life prediction of the Fe/P-BT interface was made based on the diffusion kinetics.

1 Experimental

The commercial $Bi_{0.5}Sb_{1.5}Te_3$ ingot (Ferrotec) was crushed and ground into fine powder. Fe (99.9+%, 0.68 mm), Co (99.998%, 0.68 mm), Cr (99.99%, 0.25 mm), Ti (99.9%, 106 μm), Al (99.9%, 75–150 μm), Zr (99.9%, 150 μm) were selected as the barrier layer candidates. Each of the barrier layer candidates taking up about 1wt%, were added into the P-BT powders and mixed manually for uniform dispersion. Then the mixed powder was loaded into a graphite mold, and co-sintered in a spark plasma sintering system (SPS-5000) at 420 ℃ under a pressure of 60 MPa and held for 10 min to afford densified samples containing corresponding micro-interfaces.

To fabricate TE elements, an appropriate amount of P-BT powder (~2.2 g) and Fe powder (~0.1 g) were loaded into a graphite mold as two layers and sintered by spark plasma sintering. The sintered samples were cut into rectangular Fe/P-BT TE elements with a cross-sectional area of 3 mm×3 mm. The aging samples were sealed in quartz tubes under vacuum, and then placed in a furnace for accelerated isothermal aging. The accelerated aging temperatures were set to be 300, 325, and 350 ℃, respectively. The interfacial microstructure was characterized with a field emission scanning electron microscopy (SEM, Zeiss Spura 55, Carl Zeiss SMT, Germany). The chemical composition around the interface was analyzed using an Energy Dispersive Spectrometer (OXFORD, X-MaxN, Oxfordshire, UK). The interfacial resistivity was measured with the four-probe method reported in ref.[32]. All data of the diffusion layer thickness and the interfacial resistivity in this study are the average of three parallel samples.

2 Results and discussion

2.1 High-throughput screening of the barrier layer candidates

By co-sintering the mixed powders, various micro-interfaces between P-BT matrix and 6 kinds of barrier layer candidate particles were integrated into one single sample, as shown in Fig. 1. The sample was then aged at 300 ℃ for 2 d. Fig. 2 exhibits the surface mappings of the 6 aged micro-interfaces.

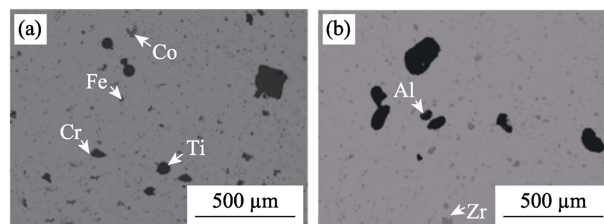

Fig. 1 Low magnification SEM images of the micro-interfaces in the as-prepared co-sintered sample for screening of the barrier layer materials

(a) Cr, Fe, Co, Ti; (b) Al, Zr

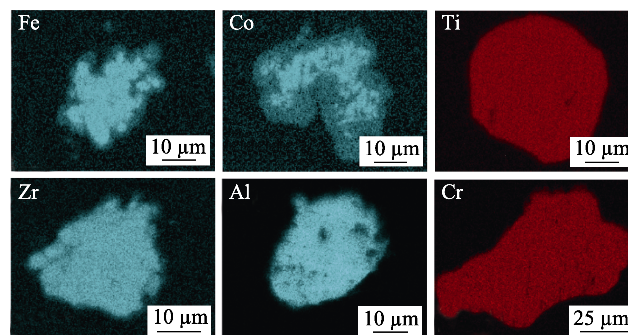

Fig. 2 Surface mapping of the micro-interfaces between P-BT matrix and 6 barrier layer candidate particles aged at 300 ℃ for 2 d

After being aged at 300 ℃ for 2 d, obvious diffusion layers appear at the Fe/P-BT and Co/P-BT interfaces. The diffusion layer thickness of the Co/P-BT interface is thicker than that of Fe/P-BT. The inter-diffusion at the other interfaces can be almost ignored. From this perspective, Fe should be the most suitable barrier layer material in the above 6 candidates. Meanwhile, Fe is cheap and owns a matched thermal expansion coefficient with P-BT matrix. As a result, Fe was screened out as the preferred barrier layer material for P-BT.

2.2 Interfacial evolution of the Fe/P-BT elements

Fe/P-BT TE elements with a cross-sectional area of 3 mm×3 mm were prepared. Microstructures and chemical compositions at the interface before and after aging were studied. As shown in Fig. 3(a), the sintered Fe/P-BT interface before aging is well bonded, but the interfacial structure is complicated. There is a clear intermediate region between the Fe barrier layer and the P-BT matrix. We confirmed that the darker part of the intermediate region adjacent to Fe is $Fe_{36}Sb_{23}Te_{41}$ from the line scanning of the interface shown in Fig. 3(b). According to ref. [33], it is the ternary Fe-Sb-Te phase compound, which is the diffusion layer resulting from the diffusion of some Sb and Te atoms in the interfacial P-BT matrix into the Fe barrier layer. The brighter part of the intermediate region adjacent to the P-BT matrix is $Bi_{20}Sb_{25}Te_{55}$. This is most likely a transitional zone with the same structure of the P-BT matrix and increased Bi content, which is transformed from the interfacial P-BT matrix when part of its internal Sb and Te atoms move out into the Fe barrier layer. Then the morphology of the Fe/P-BT interface after aging was investigated. As a typical example, Fig. 4 demonstrates the evolution of the Fe-Sb-Te diffusion layer and the Bi-rich transitional zone at the Fe/P-BT interface during aging at 275 and 350 ℃. With the aging time prolonging and the temperature increasing, the Fe-Sb-Te diffusion layer gradually grows, and its composition remains basically unchanged. While for the transitional zone, the situation is more complicated. With the aging time prolonging and the temperature increasing, the transitional zone grows thicker, but its thickness becomes increasingly uneven. Finally, the continuity of the transitional zone is destroyed. After being aged at 350 ℃ for 9 d(Fig. 4(a-d)), it transforms from a continuous layer into a number of zones dispersing as far as 20 μm inside the interfacial P-BT matrix. It's worth mentioning that of the composition of the transitional zone after aging can still be expressed as $Bi_xSb_{45-x}Te_{55}$(x>15) despite the great changes of its morphology.

2.3 Diffusion kinetics of the Fe/P-BT interface

Based on the evolution of the Fe/P-BT interfacial microstructure during accelerated aging, we studied the corresponding diffusion kinetics. Fig. 5(a) shows the relationship between the diffusion layer thickness and the square root of the aging time at different temperatures. They are linearly related, indicating that the evolution of the diffusion layer is controlled by diffusion process.

By linearly fitting the diffusion layer thickness with the square root of the aging time, its growth rates (D) at 300, 325, and 350 ℃ are obtained respectively. As shown in Fig. 5(b), according to the linear fitting of ln$D$ with 1000/T from the transformed Arrhenius formula[34]:

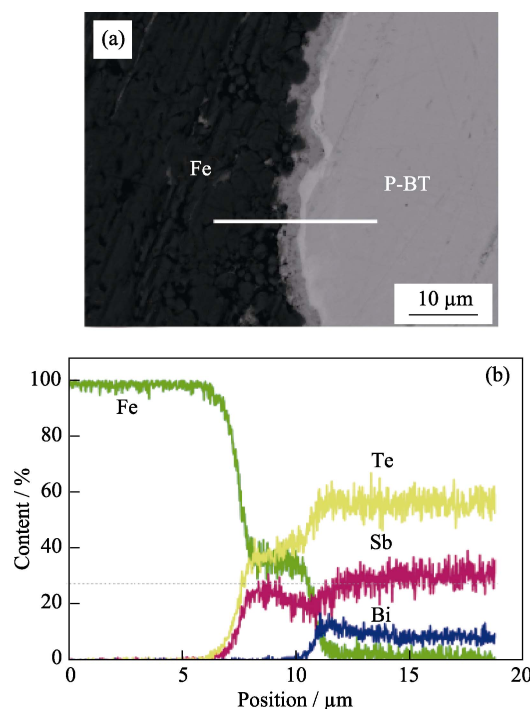

Fig. 3 (a) Interfacial microstructure of the as-prepared Fe/P-BT TE element before aging and (b) line scanning of the as-prepared Fe/P-BT interface

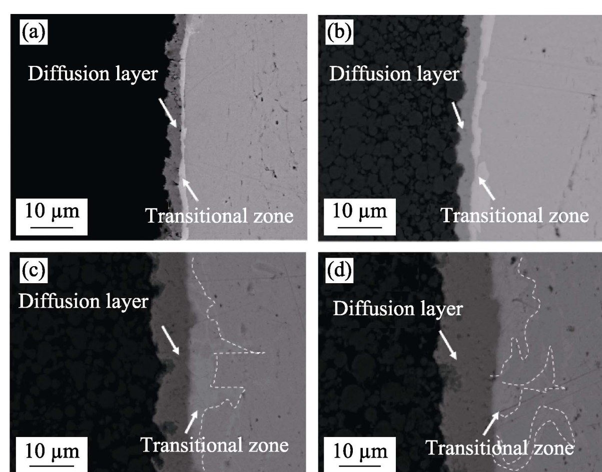

Fig. 4 Cross sectional microstructures of the Fe/P-BT interface after aging at different temperatures for different time
(a) 275 ℃, 4 d; (b) 275 ℃, 9 d; (c) 350 ℃, 4 d; (d) 350 ℃, 9 d

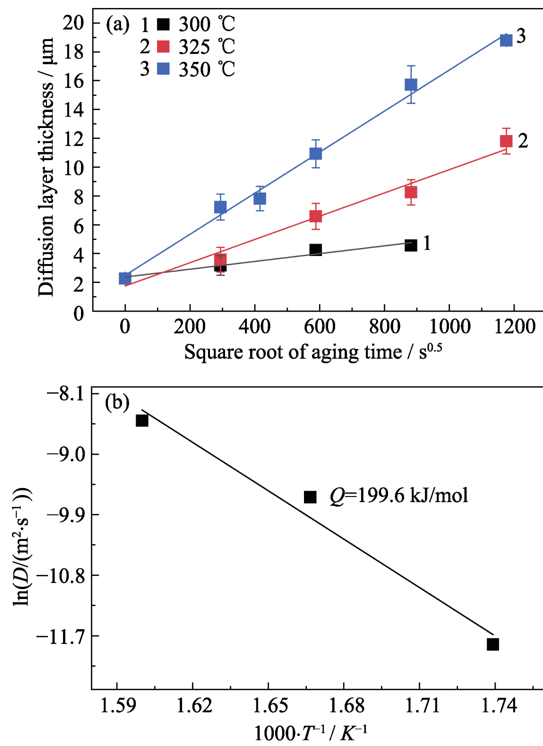

Fig. 5 (a) Variation of the diffusion layer thickness at the Fe/P-BT interface with the square root of aging time at 300, 325 and 350 ℃, and (b) variation of ln$D$ with 1000/T between 300 and 350 ℃

$$\ln D = -\frac{Q}{1000R}\frac{1000}{T} + D_0 \qquad (1)$$

where D_0 is the growth constant, Q is the growth activation energy of the diffusion layer, T is the Calvin temperature, and R is the gas constant. The growth activation energy of the diffusion layer was figured out to be 199.6 kJ/mol in the temperature range from 300 to 350 ℃.

2.4 Stability of the Fe/P-BT interfacial resistivity

At the same time, we also measured the interfacial resistivity of the Fe/P-BT elements using the four-probe method. It was found that the initial interfacial resistivity was lower than 1 μΩ·cm^2. This result indicates that good contacts form during sintering between the Fe barrier layer, the Fe-Sb-Te diffusion layer, the transitional zone and the P-BT matrix. Fig. 6 presents the variation of the interfacial resistivity with aging time at 350 ℃. During aging, the interfacial resistivity increases slowly and shows a tendency of saturation. After being aged for 16 d at 350 ℃, it is still below 10 μΩ·cm^2. This implies that the essence of the interfacial contacts remains unchanged during aging.

For an intact interfacial structure, during short-term aging, the formation of the interfacial diffusion layers may change the essence of the interfacial contact and result in dramatic variation of the interfacial resistivity. In addition, the growth of the interfacial diffusion layers introduces additional resistance. These are the main contributors for the increase of the interfacial resistivity. Furthermore, excessive growth of the interfacial diffusion layers may lead to interfacial structural defects like micro-cracks and holes, which are the main reasons of some abnormal variations of the interfacial resistivity during long-term aging.

As the essence of the interfacial contacts remains unchanged during aging, and according to Fig. 4(d), the micro-structure at the Fe/P-BT interface remains intact, we can affirm that the interfacial resistivity is mainly related to the growth of the interfacial diffusion layers. So the evolution of the interfacial resistivity of the Fe/P-BT interface during long-term aging can be analyzed based on the growth kinetics of the diffusion layer in 2.3. Assuming that the Fe/P-BT interface fails when the interfacial resistivity exceeds 10 μΩ·cm^2. Then its service life at 350 ℃ is not less than 16 d, and the corresponding diffusion layer thickness is not less than 18.8 μm. Based on the results of the diffusion kinetics in Table 1, the service life of the Fe/P-BT interface at 300 ℃ is longer than 428 d. Considering that the possible hot side working temperature of bismuth telluride TE devices (250–275 ℃) should be evidently lower than 300 ℃, the practical service life of the Fe/P-BT interface can be

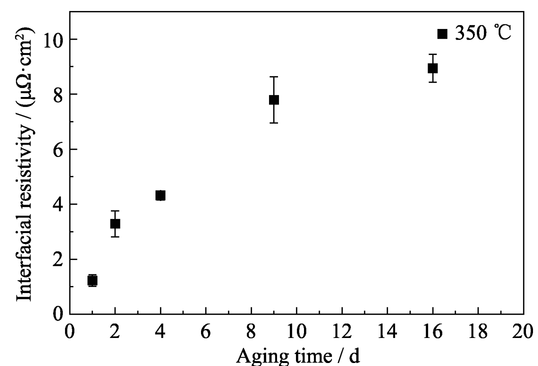

Fig. 6 Evolution of the Fe/P-BT interfacial resistivity with aging time at 350 ℃

Table 1 Fitting results of the growth rates of the diffusion layers, the relationship between diffusion layer thickness and aging time, and predicted service lives of the Fe/P-BT element at different temperatures

Temperature/ ℃	D/(×10^{-18}, m^2·s^{-1})	$(Y-Y_0)$/μm	Predicted service life*/d
300	7.29	$2.7\times10^{-3}t^{0.5}$	428
325	65.1	$8.1\times10^{-3}t^{0.5}$	52
350	203.1	$14.3\times10^{-3}t^{0.5}$	16

* The prediction is based on the assumption that a Fe/P-BT element fails when the interfacial diffusion layer thickness reaches 18.8 μm

extended significantly. Based on the above results, it is concluded that Fe is a promising barrier layer material of the P-BT TE devices for high temperature power generation.

3 Conclusion

In this study, Fe was screened out from 6 candidates as the barrier layer material for $Bi_{0.5}Sb_{1.5}Te_3$. Fe/P-BT thermoelectric elements were fabricated by one-step spark plasma sintering and aged at 300, 325 and 350 ℃ to evaluate the high temperature interfacial stability. It is found that during sintering, a ternary phase diffusion layer of $Fe_{36}Sb_{23}Te_{41}$ forms adjacent to Fe barrier layer, while a transitional zone of $Bi_xSb_{45-x}Te_{55}$ (x>15) forms adjacent to the P-BT matrix. During accelerated aging, the composition of the Fe-Sb-Te diffusion layer remains basically unchanged. Its thickness increases linearly with the square root of the aging time. The composition of the Bi-rich transitional zone is still expressed as $Bi_xSb_{45-x}Te_{55}$ (x>15), but its morphology changes greatly. After being aged for 9 d at 350 ℃, the separated transitional zones stretched nearly 20 μm into the P-BT matrix. The interfacial resistivity was lower than 1 $\mu\Omega\cdot cm^2$ and increased slowly during the aging process. Life prediction based on the diffusion kinetics of the Fe/P-BT interface shows that the Fe/P-BT TE element has a promising application at the temperature below 300 ℃.

References:

[1] ZHANG Q H, HUANG X Y, BAI S Q, *et al*. Thermoelectric devices for power generation: recent progress and future challenges. *Advanced Engineering Materials*, 2016, **18(2):** 194–213.

[2] SHI X, CHEN L, UHER C. Recent advances in high-performance bulk thermoelectric materials. *International Materials Reviews*, 2016, **61(6):** 379–415.

[3] LU Z, ZHANG H, MAO C, *et al*. Silk fabric-based wearable thermoelectric generator for energy harvesting from the human body. *Applied Energy*, 2016, **164:** 57–63.

[4] ZEBARJADI M, ESFARJANI K, DRESSELHANS M, *et al*. Perspectives on thermoelectrics: from fundamentals to device applications. *Energy Environmental Science*, 2012, **5(1):** 5147–5162.

[5] ZHU T J. Recent advances in thermoelectric materials and devices. *Journal of Inorganic Materials*, 2019, **34(3):** 233–236.

[6] ZHANG Q H, BAI S Q, CHEN L D. Technologies and applications of thermoelectric devices: current status, challenges and prospects. *Journal of Inorganic Materials*, 2019, **34(3):** 0279–0294.

[7] HAO F, QIU P F, TANG Y S, *et al*. High efficiency Bi_2Te_3-based materials and devices for thermoelectric power generation between 100 and 300 ℃. *Energy Environmental Science*, 2016, **9(10):** 3120–3127.

[8] YOON S M, DHARMAIAH P, KIM H S, *et al*. Investigation of thermoelectric properties with dispersion of Fe_2O_3 and Fe-85Ni nanospheres in $Bi_{0.5}Sb_{1.5}Te_3$ matrix. *Journal of Electronic Materials*, 2017, **46(5):** 2770–2777.

[9] SHEN J, YIN Z, YANG S, *et al*. Improved thermoelectric performance of p-type bismuth antimony telluride bulk alloys prepared by hot forging. *Journal of Electronic Materials*, 2011, **40(5):** 1095–1099.

[10] HU L, GAO H, LIU X, *et al*. Enhancement in thermoelectric performance of bismuth telluride based alloys by multi-scale microstructural effects. *Journal of Materials Chemistry A*, 2012, **22(32):** 16484–16490.

[11] FAN J F, CHEN L F, BAI S Q, *et al*. Joining of Mo to $CoSb_3$ by spark plasma sintering by inserting a Ti interlayer. *Materials Letters*, 2004, **58(30):** 3876–3878.

[12] TANG Y S, BAI S Q, REN D D, *et al*. Interface structure and electrical property of $Yb_{0.3}Co_4Sb_{12}$/Mo-Cu element prepared by welding using Ag-Cu-Zn solder. *Journal of Inorganic Materials*, 2015, **30(3):** 256–260.

[13] LIU W S, LIU Y, ZHE F, *et al*. Thermoelectric device: contact interface and interface materials. *Journal of Inorganic Materials*, 2019, **34(3):** 0269–0279.

[14] ZHAO D G, WANG L, CAI Y H, *et al*. One-step Sintering of $CoSb_3$ Thermoelectric Material and Cu-W Alloy By Spark Plasma Sintering. Materials Science Forum, Switzerland, 2009, **610:** 389–393.

[15] ZHAO D G, LI X Y, HE L, *et al*. Interfacial evolution behavior and reliability evaluation of $CoSb_3$/Ti/Mo-Cu thermoelectric joints during accelerated thermal aging. *Journal of Alloys and Compounds*, 2009, **477(1/2):** 425–431.

[16] GU M, XIA X G, LI X, *et al*. Microstructural evolution of the interfacial layer in the Ti-Al/$Yb_{0.6}Co_4Sb_{12}$ thermoelectric joints at high temperature. *Journal of Alloys and Compounds*, 2014, **610:** 665–670.

[17] CHEN S W, WU C Y, WU H J, *et al*. Interfacial reactions in Sn/Bi_2Te_3, Sn/Bi_2Se_3 and Sn/$Bi_2(Te_{1-x}Se_x)_3$ couples. *Journal of Alloys and Compounds*, 2014, **611:** 313–318.

[18] CHEN S W, CHIU C N. Unusual cruciform pattern interfacial reactions in Sn/Te couples. *Scripta Materialia*, 2007, **56(2):** 97–99.

[19] LAN Y C, WANG D Z, CHEN G, *et al*. Diffusion of nickel and tin in p-type $(Bi,Sb)_2Te_3$ and n-type $Bi_2(Te,Se)_3$ thermoelectric materials. *Applied Physics Letters*, 2008, **92(10):** 101910.

[20] CHEN L Q, MEI D Q, WANG Y C, *et al*. Ni barrier in Bi_2Te_3-based thermoelectric modules for reduced contact resistance and enhanced power generation properties. *Journal of Alloys and Compounds*, 2019, **796:** 314–320.

[21] CHEN S W, YANG T R, WU C Y, *et al*. Interfacial reactions in the Ni/$(Bi_{0.25}Sb_{0.75})_2Te_3$ and Ni/$Bi_2(Te_{0.9}Se_{0.1})_3$ couples. *Journal of Alloys and Compounds*, 2016, **686:** 847–853.

[22] LIU W, WANG H, WANG L, *et al*. Understanding of the contact of nanostructured thermoelectric n-type $Bi_2Te_{2.7}Se_{0.3}$ legs for power generation applications. *Journal of Materials Chemistry A*, 2013, **1(42):** 13093–13100.

[23] FENG S P, CHANG Y H, YANG J, *et al*. Reliable contact fabrication on nanostructured Bi_2Te_3-based thermoelectric materials. *Phys. Chem. Chem. Phys.*, 2013, **15(18):** 6757–6762.

[24] LIN W C, LI Y S, WU A T. Study of diffusion barrier for solder/*n*-Type Bi_2Te_3 and bonding strength for p- and n-type thermoelectric modules. *Journal of Electronic Materials*, 2017, **47(1):** 148–154.

[25] SONG E, SWRTZENTRUBER B S, KORIPELLA C R, *et al*. Highly effective GeNi alloy contact diffusion barrier for BiSbTe long-term thermal exposure. *ACS Omega*, 2019, **4(5):** 9376–9382.

[26] WANG C H, HEIEH H C, LEE H Y, *et al*. Co-P diffusion barrier for p-Bi_2Te_3 thermoelectric material. *Journal of Electronic Materials*, 2018, **48(1):** 53–57.

[27] LIN W P, WESOLOWSKI D E, LEE C C. Barrier/bonding layers on bismuth telluride (Bi_2Te_3) for high temperature thermoelectric modules. *Journal of Materials Science: Materials in Electronics*,

2011, **22(9):** 1313–1320.

[28] HSU H H, CHENG C H, LIN Y L, *et al*. Structural stability of thermoelectric diffusion barriers: experimental results and first principles calculations. *Applied Physics Letters*, 2013, **103(5):** 053902.

[29] BAE N H, HAN S, LEE K E, *et al*. Diffusion at interfaces of micro thermoelectric devices. *Current Applied Physics*, 2011, **11(5):** 40–44.

[30] KACSICH T, KOLAWA E, FLEURIAL J, *et al*. Films of Ni-7at% V, Pd, Pt and Ta-Si-N as diffusion barriers for copper on. *Journal of Physics D: Applied Physics*, 1998, **31(19):** 2406–2409.

[31] GU M, BAI S Q, WU J, *et al*. A high-throughput strategy to screen interfacial diffusion barrier materials for thermoelectric modules. *Journal of Materials Research*, 2019, **34(7):** 1179–1187.

[32] GU M, XIA X, HUANG X, *et al*. Study on the interfacial stability of p-type Ti/$Ce_yFe_xCo_{4-x}Sb_{12}$ thermoelectric joints at high temperature. *Journal of Alloys Compounds*, 2016, **671:** 238–244.

[33] YAMAGUCHI G, SHIMADA M, KOIZUMI M, *et al*. Preparation and characterization of compounds of the system $Fe(Sb_{1-x}Te_x)_2$ ($0 \leqslant x \leqslant 1.0$). *Journal of Solid State Chemistry*, 1980, **34(2):** 241–245.

[34] ZHANG G H, LIAO J C, TANG Y S, *et al*. Interface stability of skutterudite thermoelectric materials/$Ti_{88}Al_{12}$. *Journal of Inorganic Materials*, 2018, **33(8):** 889–894.

$Fe/Bi_{0.5}Sb_{1.5}Te_3$热电元件高温稳定性研究

王 旭[1,2], 顾 明[1], 廖锦城[1], 宋庆峰[1], 史 迅[1], 柏胜强[1], 陈立东[1,2]

(1. 中国科学院 上海硅酸盐研究所, 高性能陶瓷和超微结构国家重点实验室, 上海 201899; 2. 中国科学院大学材料科学与光电技术学院, 北京 100049)

摘 要: 热电元件的界面高温稳定性是决定热电器件服役性能和应用前景的重要因素, 而阻挡层和热电材料之间的界面扩散和界面电阻则是评价热电元件高温稳定性的主要标准。为了进一步提升 P 型碲化铋热电器件的界面稳定性, 本研究采用高通量筛选的方法选定适用于 P 型碲化铋的 Fe 阻挡层材料。通过一步烧结的方法制备了 Fe/P-BT 的热电元件, 并系统研究了高温加速老化实验下的 Fe/P-BT 的界面微观结构的演变和界面电阻率的稳定性。在老化过程中, Fe/P-BT 的界面连接良好且 Fe-Sb-Te 的三元扩散层的成分基本不变。扩散层厚度与时间的平方根成线性关系, 生长激活能为 199.6 kJ/mol。Fe/P-BT 的界面电阻率较小且随着老化时间延长缓慢增大, 在 350 ℃老化 16 d 后仍然低于 10 μΩ·cm^2。基于界面扩散动力学的寿命预测表明 Fe 可以用作 $Bi_{0.5}Sb_{1.5}Te_3$ 热电元件的阻挡层材料。

关 键 词: 热电元件; 碲化铋; 阻挡层; 界面扩散; 界面电阻率

中图分类号: TQ174 **文献标识码:** A